Article

Reversible Dimerization of [5,6]-CO

Dmitri Tsyboulski, Dieter Heymann, Sergei M. Bachilo, Lawrence B. Alemany, and R. Bruce Weisman

J. Am. Chem. Soc., **2004**, 126 (23), 7350-7358• DOI: 10.1021/ja048937d • Publication Date (Web): 22 May 2004

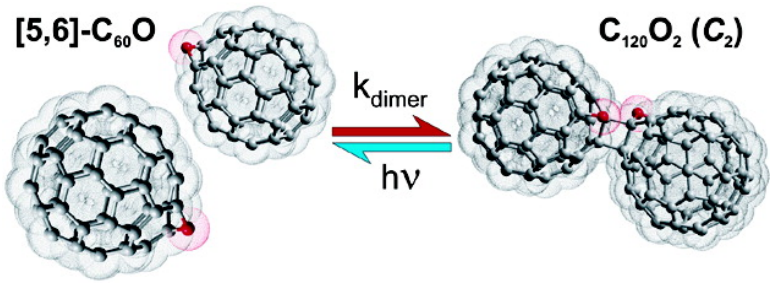

More About This Article

Additional resources and features associated with this article are available within the HTML version:

- Supporting Information
- Access to high resolution figures
- Links to articles and content related to this article
- Copyright permission to reproduce figures and/or text from this article

View the Full Text HTML

J|A|C|S
ARTICLES
Published on Web 05/22/2004

Reversible Dimerization of [5,6]-$C_{60}O$

Dmitri Tsyboulski,[†] Dieter Heymann,[‡] Sergei M. Bachilo,[†]
Lawrence B. Alemany,[†] and R. Bruce Weisman*,[†]

Contribution from the Department of Chemistry and Department of Earth Science, and Center for Nanoscale Science and Technology, Rice University, 6100 Main Street, Houston, Texas 77005

Received February 25, 2004; E-mail: weisman@rice.edu

Abstract: The recently discovered [5,6]-open isomer of $C_{60}O$ has been found to undergo facile dimerization to form a new C_2 symmetry isomer of $C_{120}O_2$, which can be photodissociated with relatively high efficiency to regenerate monomeric [5,6]-$C_{60}O$. High yield dimerization of [5,6]-$C_{60}O$ proceeds spontaneously in toluene solution near room temperature. On the basis of ^{13}C NMR spectroscopy, ab initio quantum computations, and HPLC retention patterns, the resulting $C_{120}O_2$ product has been deduced to be a nonpolar dimer of C_2 symmetry in which the $C_{60}O$ moieties are linked by two single bonds between sp^3-hybridized carbon atoms adjacent to oxygen atoms. Photophysical properties of this dimer have also been measured and compared to those of C_{120}, the [2 + 2]-dimer of C_{60}. The ground-state absorption spectrum of $C_{120}O_2$ in toluene is slightly red-shifted relative to that of C_{120}, with a distinctive peak at 329 nm and an S_1-S_0 origin band at 704 nm. Its fluorescence spectrum shows two major peaks at 718 and 793 nm. In room-temperature toluene, the measured triplet state intrinsic lifetime of this $C_{120}O_2$ isomer is 34 ± 2 μs, a value somewhat shorter than that of C_{120} (44 μs). $C_{120}O_2$ undergoes photodissociation from its triplet state to regenerate monomeric [5,6]-$C_{60}O$ with quantum yields of 2.5% at 24 °C and 43% at 70 °C. It can therefore serve as a stable reactant for photolytic production of [5,6]-$C_{60}O$. As a simple fullerene adduct that reacts under mild conditions, [5,6]-$C_{60}O$ may prove useful in special synthetic applications. Solutions of [5,6]-$C_{60}O$ are also unique because they can provide mixtures of a fullerene monomer and its dimer in a dynamic balance controllable by adjustment of concentration, temperature, and optical irradiation.

Introduction

Fullerene dimers hold special interest because their properties can reveal interactions between the component fullerene moieties and also because they may play important roles as intermediates in fullerene polymerizations.[1] The most basic fullerene dimer may be considered the dumbbell-shaped C_{120} molecule, which was first synthesized through a KCN-catalyzed mechanochemical [2 + 2] cycloaddition reaction of C_{60}.[2,3] Many properties of C_{120} have been characterized in subsequent studies.[4−9] Intense interest in fullerene oxides, which are among the first known fullerene derivatives,[10] had earlier led to the finding that [6,6]-$C_{60}O$ (an epoxide) reacts with C_{60} near 200 °C to form $C_{120}O$, an oxygen-bridged dimer containing a furan linkage between the fullerene cages.[11,12] This product was also found to be produced through the ambient temperature solid-state reaction of [6,6]-$C_{60}O$ with C_{60}.[13] A dimeric fullerene oxide with the formula $C_{120}O_2$ was first prepared by Gromov et al. through the 400 °C thermolysis of solid $C_{120}O$.[14] This species was found to have C_{2v} symmetry and two furanoid bridges linking the fullerene cages; it has since been the subject of various experimental and theoretical investigations.[6,13,15−23] Two

[†] Department of Chemistry and Center for Nanoscale Science and Technology.
[‡] Department of Earth Science.

(1) Segura, J. L.; Martin, N. *Chem. Soc. Rev.* **2000**, *29*, 13−25.
(2) Wang, G.-W.; Komatsu, K.; Murata, Y.; Shiro, M. *Nature* **1997**, *387*, 583−586.
(3) Komatsu, K.; Wang, G.-W.; Murata, Y.; Tanaka, T.; Fujiwara, K.; Yamamoto, K.; Saunders, M. *J. Org. Chem.* **1998**, *63*, 9358−9366.
(4) Osawa, S.; Sakai, M.; Osawa, E. *J. Phys. Chem. A* **1997**, *101*, 1378−1383.
(5) Ma, B.; Riggs, J. E.; Sun, Y.-P. *J. Phys. Chem. B* **1998**, *102*, 5999−6009.
(6) Lebedkin, S.; Gromov, A.; Giesa, S.; Gleiter, R.; Renker, B.; Rietschel, H.; Krätschmer, W. *Chem. Phys. Lett.* **1998**, *285*, 210−215.
(7) Fujitsuka, M.; Luo, C.; Ito, O.; Murata, Y.; Komatsu, K. *J. Phys. Chem. A* **1999**, *103*, 7155−7160.
(8) Cho, H. S.; Kim, S. K.; Kim, D.; Fujiwara, K.; Komatsu, K. *J. Phys. Chem. A* **2000**, *104*, 9666−9669.
(9) Bachilo, S. M.; Benedetto, A. F.; Weisman, R. B. *J. Phys. Chem. A* **2001**, *105*, 9845−9850.
(10) Creegan, K. M.; Robbins, J. L.; Robbins, W. K.; Millar, J. M.; Sherwood, R. D.; Tindall, P. J.; Cox, D. M.; Smith, A. B., III.; McCauley, J. P., Jr.; Jones, D. R.; Gallagher, R. T. *J. Am. Chem. Soc.* **1992**, *114*, 1103−1105.
(11) Smith, A. B., III; Tokuyama, H.; Strongin, R. M.; Furst, G. T.; Romanow, W. J. *J. Am. Chem. Soc.* **1995**, *117*, 9359−9360.
(12) Lebedkin, S.; Ballenweg, S.; Gross, J.; Taylor, R.; Krätschmer, W. *Tetrahedron Lett.* **1995**, *36*, 4971−4974.
(13) Taylor, R.; Barrow, M. P.; Drewello, T. *Chem. Commun.* **1998**, 2497−2498.
(14) Gromov, A.; Lebedkin, S.; Ballenweg, S.; Avent, A. G.; Taylor, R.; Krätschmer, W. *Chem. Commun.* **1997**, 209−210.
(15) Fowler, P. W.; Mitchell, D.; Taylor, R.; Seifert, G. *J. Chem. Soc., Perkin Trans. 2* **1997**, 1901−1905.
(16) Penn, S. G.; Costa, D. A.; Balch, A. L.; Lebrilla, C. B. *Int. J. Mass Spectrom. Ion Processes* **1997**, *169/170*, 371−386.
(17) Eisler, H.-J.; Hennrich, F. H.; Werner, E.; Hertwig, A.; Stoermer, C.; Kappes, M. M. *J. Phys. Chem. A* **1998**, *102*, 3889−3897.
(18) Krause, M.; Dunsch, L.; Seifert, G.; Fowler, P. W.; Gromov, A.; Krätschmer, W.; Gutierez, R.; Porezag, D.; Frauenheim, T. *J. Chem. Soc., Faraday Trans.* **1998**, *94*, 2287−2294.
(19) Gross, J. H.; Giesa, S.; Krätschmer, W. *Rapid Commun. Mass Spectrom.* **1999**, *13*, 815−820.
(20) Tian, W.; Ren, A.; Feng, J.; Guo, J.; Sun, C. *Int. J. Quantum Chem.* **2000**, *79*, 291−307.

10.1021/ja048937d CCC: $27.50

additional$C_{120}O_2$ isomers of C_1 symmetry are reportedly formed as byproducts in the 200 °C solid-state reaction between C_{60} and $C_{60}O$.[24]

A recent study in this laboratory uncovered a new isomer of $C_{60}O$, the [5,6]-open oxidoannulene (oxa-homo[60]fullerene), which can be simply produced through photolysis of the ozonide $C_{60}O_3$. Following up on a preliminary report,[25] we describe here a dimerization reaction of this [5,6]-$C_{60}O$ species that proceeds in room-temperature solution to form a new isomer of $C_{120}O_2$. This is apparently the most facile reaction yet found for producing a fullerene dimer. We also report the structural characterization and photophysical properties of the $C_{120}O_2$ isomer formed by dimerization. Most intriguingly, our $C_{120}O_2$ has been found to photodissociate with relatively high efficiency to regenerate the [5,6]-$C_{60}O$ monomer. The [5,6]-$C_{60}O$/$C_{120}O_2$ system thus provides the first example of reversible fullerene dimerization.

Experimental Methods

Synthesis. We synthesized $C_{120}O_2$ through thermal dimerization of [5,6]-open $C_{60}O$ (oxa-homo[60]fullerene). The $C_{60}O$ reactant was prepared according to the procedure in a recent report by treating a ~2.5 mM solution of C_{60} in *o*-xylene with a stream of O_3 in O_2 from a discharge ozone generator (Ozone Services GE60).[26] The resulting $C_{60}O_3$ adduct was isolated on a Shimadzu HPLC equipped with a SPD-M10A photodiode array detector and a semipreparative Cosmosil 5PYE column that was cooled to 0 °C. The mobile phase was toluene. Immediate irradiation of this fraction with an incandescent light source photolyzed the $C_{60}O_3$ to produce O_2 and [5,6]-open $C_{60}O$.

The dimerization reaction was induced simply by evaporating the toluene solution of [5,6]-open $C_{60}O$ to higher concentration or dryness using rotary evaporation at 40 °C under partial vacuum. After the resulting solid was redissolved in toluene, $C_{120}O_2$ product was isolated and purified by HPLC using the Cosmosil 5PYE column.

^{13}C NMR Spectroscopy. The solubility of $C_{120}O_2$ in ODCB-d_4 was sufficiently high (~1.4 mg/mL) to allow obtaining a ^{13}C NMR spectrum with a 5 mm broadband observe (BBO) probe on a Bruker Avance500 spectrometer (^{1}H = 500.13 MHz, ^{13}C = 125.77 MHz). The solution contained 1.1 mg of 4% ^{13}C-enriched sample, along with 10 mg of $Cr(acac)_3$ as a paramagnetic relaxation agent and 10 μL of TMS as a chemical shift reference. A plastic vortex plug was placed in the sample tube just above the solution to prevent solvent evaporation during the experiment, as a change in concentration would broaden each signal by slightly changing the chemical shift. Preliminary ^{1}H NMR spectra were obtained to guide shimming until a TMS half-height line width of 0.31 Hz was achieved. A ^{13}C NMR spectrum covering the region from 166.6 ppm to −3.3 ppm was then obtained with a 1.9 μs 30° pulse, a 3.067 s FID with WALTZ ^{1}H decoupling, and a 4 s relaxation delay without decoupling (so as to minimize the NOE for the residual 1% ODCB-hd_3 ^{13}C signals). The sample was kept at 30 °C throughout the experiment to prevent precipitation. A total of 48 856 scans were taken over a 96 h period. To reduce high frequency noise, the FID was processed with only 0.1 Hz of line broadening, as the digital resolution was 0.326 Hz (0.00259 ppm). The relative peak heights give only a qualitative indication of intensity because the line widths (and thus peak heights) do not have to be identical for the 60 different ^{13}C signals. Even in the presence of a paramagnetic relaxation agent, the different ^{13}C environments may not relax equally during the 4-s relaxation delay.

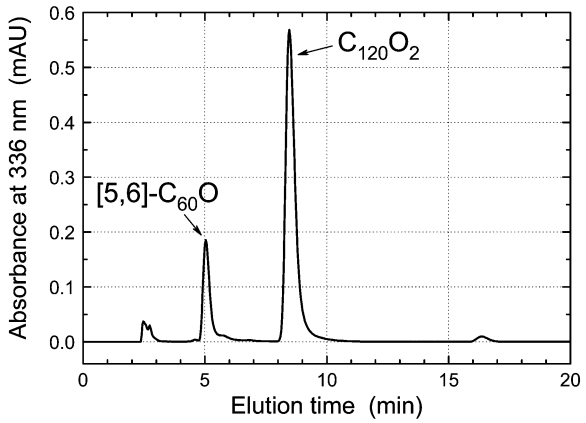

Figure 1. Chromatogram of the evaporated and redissolved [5,6]-$C_{60}O$.

Mass Spectrometry. Two different mass spectrometry methods were applied in this project. MALDI-TOF analysis was performed with a Bruker Biflex III instrument using 9-nitroanthracene as a matrix. APCI measurements were made on a Finnigan MAT 95 instrument.

Photophysical Measurements. Ground-state UV−vis absorption spectra were measured with a Cary 400 spectrophotometer. Fluorimetry studies were performed on a Spex Fluorolog 3-211 instrument equipped with a Hamamatsu R636-10 photomultiplier. We made transient absorption measurements using a homemade apparatus that employed 532 nm pulses from a small Q-switched Nd:YAG laser for excitation and monochromated light from a stabilized tungsten−halogen lamp for probing. An amplified silicon or germanium photodiode served as the detector. A Tektronix TDS-430A digitizing oscilloscope recorded output signals from the detector and averaged them over multiple excitation shots. Waveform data were analyzed on laboratory computers after transfer through a GPIB interface.

Quantum Chemical Computations. All computations were performed using Gaussian 98W Revision A.11.2.[27] Molecular geometries and relative energies were obtained using the AM1 and PM3 semiempirical methods and the B3LYP density functional method with various basis sets. To compute ^{13}C NMR chemical shifts, we used the GIAO method at different levels of theory. Many of these computations required one to two weeks of execution time per species on an Athlon MP 1.2 GHz workstation.

Results and Discussion

Dimerization Reaction. Figure 1 shows a chromatogram of the mixture formed by evaporating a solution of [5,6]-$C_{60}O$ to dryness near room temperature and then redissolving in toluene. In addition to the peak near the 5 min retention time from unreacted [5,6]-$C_{60}O$, there is a major peak at 8.4 min attributed to a $C_{120}O_2$ dimeric product. Up to 60% conversion of monomer was seen. Minor peaks at longer retention times, such as the one near 16.3 min, probably represent higher oligomers. To

(21) Du, S.; Huang, Y.; Li, Y.; Liu, R. *Chin. Sci. Bull.* **2001**, *46*, 818−823.
(22) Krätschmer, W. *AIP Conf. Proc. (Nanonetwork Materials)* **2001**, *590*, 291−296.
(23) Dunsch, L.; Rapta, P.; Gromov, A.; Stasko, A. *J. Electroanal. Chem.* **2003**, *547*, 35−43.
(24) Gromov, A.; Lebedkin, S.; Hull, W. E.; Krätschmer, W. *J. Phys. Chem. A* **1998**, *102*, 4997−5005.
(25) Tsyboulski, D.; Heymann, D.; Bachilo, S. M.; Alemany, L. B.; Weisman, R. B. *Proc. Electrochem. Soc.* **2002**, *2002−12*, 148−156.
(26) Weisman, R. B.; Heymann, D.; Bachilo, S. M. *J. Am. Chem. Soc.* **2001**, *123*, 9720−9721.
(27) Frisch, M. J.; Trucks, G. W.; Schlegel, H. B.; Scuseria, G. E.; Robb, M. A.; Cheeseman, J. R.; Zakrzewski, V. G.; Montgomery, J. A.; Stratmann, R. E.; Burant, J. C.; Dapprich, S.; Millam, J. M.; Daniels, A. D.; Kudin, K. N.; Strain, M. C.; Farkas, O.; Tomasi, J.; Barone, V.; Cossi, M.; Cammi, R.; Mennucci, B.; Pomelli, C.; Adamo, C.; Clifford, S.; Ochterski, J.; Petersson, G. A.; Ayala, P. Y.; Cui, Q.; Morokuma, K.; Rega, N.; Salvador, P.; Dannenberg, J. J.; Malick, D. K.; Ortiz, J. V.; Baboul, A. G.; Stefanov, B. B.; Liu, G.; Liashenko, A.; Piskorz, P.; Komaromi, I.; Gomperts, R.; Gomperts, R.; Fox, D. J.; Keith, T.; Al-Laham, M. A.; Peng, C. Y.; Nanayakkara, A.; Challacombe, M.; Gill, P. M. W.; Johnson, B.; Chen, W.; Wong, M. W.; Andres, J. L.; Gonzalez, C.; Head-Gordon, M.; Replogle, E. S.; Pople, J. A. *Gaussian 98*, revision A.11.2; Gaussian, Inc.: Pittsburgh, PA, 2001.

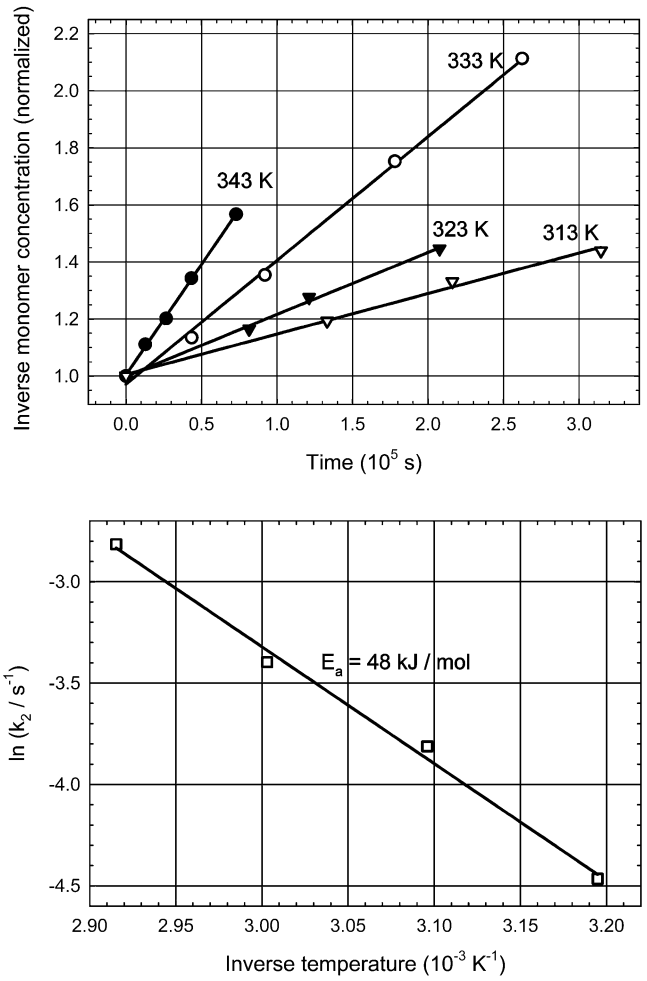

Figure 2. (Top frame) Dimerization kinetics of [5,6]-$C_{60}O$ at various temperatures. (Bottom frame) Arrhenius plot for the [5,6]-$C_{60}O$ dimerization kinetics.

study the reaction kinetics, a ca. 130 μM solution of 5,6-$C_{60}O$ was thermostated in a constant-temperature water bath and sampled at various intervals for HPLC analysis of reactant and product concentrations. The top frame of Figure 2 shows the inverse reactant concentration as a function of time as measured at four different sample temperatures. The linearity of each plot indicates pure second-order kinetics for the consumption of [5,6]-$C_{60}O$. The bimolecular rate constants found from these data are 1.2, 2.4, 3.4, and 6.0 $\times$ 10^{-2} M^{-1} s^{-1} at 40, 50, 60, and 70 °C, respectively. In the bottom frame of Figure 2, we show an Arrhenius plot of these rate constants along with a linear best-fit that indicates an overall activation energy of 48 kJ mol^{-1} for the bimolecular reaction of [5,6]-$C_{60}O$. (After correcting for the temperature-dependent viscosity of the toluene solvent, we estimate an intrinsic activation energy of 39 kJ mol^{-1}.) The dark solution-phase dimerization reaction proceeds essentially to completion, as we find an equilibrium constant for dimer formation of at least 6 $\times$ 10^9 M^{-1} in room-temperature toluene. This thermodynamic preference for dimer formation is also consistent with the quantum chemical findings reported below.

Structural Data. In an attempt to confirm the reaction product's suspected identity as $C_{120}O_2$, we performed MALDI-TOF and APCI mass spectrometry measurements. However, neither of these methods showed a signal near the expected

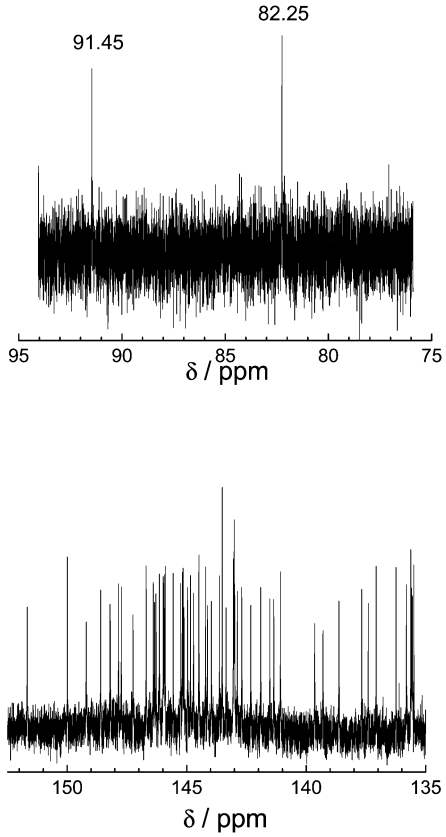

Figure 3. ^{13}C NMR spectrum of $C_{120}O_2$ in ODCB-d_4 at 30 °C showing sp^3 (top) and sp^2 regions (bottom).

parent mass of $C_{120}O_2$ (1472 amu). Instead, mass spectral signals were observed at masses 720, 736, and 752, corresponding to C_{60}, $C_{60}O$, and $C_{60}O_2$. At relatively weak MALDI-TOF excitation powers, only the $C_{60}O$ peak at 736 amu was visible. This behavior presumably reflects fragmentation of the sample compound under the influence of optical or thermal excitation. For comparison, we note that mass spectrometry of C_{120} under similar conditions also failed to show a parent peak.

As illustrated in Figure 3 and in the table in the Supporting Information, the ^{13}C NMR spectrum exhibits two sp^3 signals with nearly equal intensities at δ82.25 and δ91.45 and 56 sp^2 signals from δ151.67 to δ135.50. This pattern immediately excludes several isomers from consideration. It is clear that this compound cannot be the isomer of C_{2v} symmetry reported previously,[14,28] which ideally would give 26 double-intensity sp^2 signals, 4 single-intensity sp^2 signals, and 2 double-intensity sp^3 signals.[20] It is equally obvious that this sample is not the isomer of D_{2h} symmetry with a central cyclobutane ring and an epoxide group on the opposite side of each C_{60} moiety, as too many signals are present in our spectrum and there is no reasonable expectation that such a dimer would form from the [5,6]-open oxidoannulene $C_{60}O$. It is also apparent that our sample has far too few signals to be a C_1 symmetry isomer of $C_{120}O_2$, including either described in a prior report.[24] The measured ^{13}C NMR signals are noticeably narrower than those shown previously for C_{2v} $C_{120}O_2$,[14,28] in which only 27 of the 30 different sp^2 signals were resolved at the same field strength used here. Still, only 56 of the 58 expected sp^2 signals are clearly visible for our sample. A highly expanded plot with no line

(28) Taylor, R. *Proc. Electrochem. Soc.* **1997**, *97−14*, 281−289.

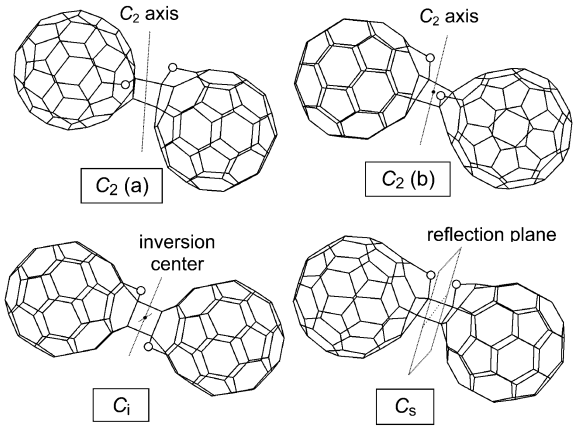

Figure 4. Possible structures of $C_{120}O_2$ having C_2, C_s, or C_i symmetries suggested by NMR results.

broadening and 4-fold zero-filling to even better define line shape clearly shows that the δ143.51 signal is both taller and broader than the adjacent signals, with an area 2 to 3 times that of the others.

The number of observed signals with similar heights indicates a single isomeric species with one symmetry element and, thus, a point group symmetry of C_2, C_s, or C_i. A compound of such symmetry would ideally give two sp^3 signals and 58 sp^2 signals of equal intensity. From the observation of two sp^3 signals with nearly equal intensity, we deduce that the $C_{60}O$ moieties are linked by two bonds involving four sp^3-hybridized carbon atoms. (A structure with one linking bond would be unstable because of radical centers; one with three bonds would not show sp^3 signals of equal intensity; and one with four bonds would show a higher ratio of sp^3 to sp^2 signals.) Although one could imagine a $C_{120}O_2$ peroxide of C_2 or C_s symmetry, we consider such a structure unlikely because it could be formed only by substantial rearrangement of the parent $C_{60}O$, giving a dimerization activation energy higher than the observed value.

Thus, we conclude that the dimer contains four sp^3 carbon atoms and retains the [5,6]-open oxidoannulene character of the monomer. Bonding between the $C_{60}O$ moieties in such structures would resemble that in C_{120}, the dumbbell-shaped dimer of C_{60} that is linked by two single bonds formed in a 2 + 2 cycloaddition process. The sp^3 chemical shift values observed for our $C_{120}O_2$ isomer suggest that those atoms are deshielded by proximity to an oxygen atom.[2,11,14,24] The most plausible structures satisfying these constraints are those with oxygen atoms directly bound to the sp^3 carbons and an overall symmetry of C_s, C_2, or C_i. Figure 4 shows these candidate structures. (Note, however, that one cannot immediately exclude other structures of these symmetries in which the oxygen atom is located one bond further away from the bridging sites.)

For any of the structures, the sp^2 carbon bound to oxygen would, of course, be much further downfield than the two sp^3 signals,[10,29] so 58 relatively deshielded ^{13}C signals would be expected for a dimeric oxidoannulene that has a rotation, reflection, or inversion symmetry element. Of the two sp^3 carbons, one could reasonably expect the one bound to oxygen to be more deshielded. In principle, the two sp^3 carbons can be unambiguously differentiated through a 2D INADEQUATE NMR experiment, as the sp^3 carbon bound to oxygen can exhibit only one connectivity to a sp^2 site. Unfortunately, the concentration of ^{13}C in the sample was far too low for this experiment to be feasible on our spectrometer.

Other C_{120} dimer structures with a central cyclobutane ring do not exhibit two such deshielded cyclobutane carbon signals, i.e., having both cyclobutane signals downfield of 82 ppm rather than at least one signal at 76 ppm or further upfield.[2,14,30−35] The difference between the more upfield sp^3 chemical shift in C_{2v} $C_{120}O_2$ and in our isomer of $C_{120}O_2$ is striking (δ72.19 vs δ82.25), whereas the difference between the more downfield sp^3 chemical shifts is much smaller (δ92.11 vs δ91.45) and in the reverse order. Clearly, the electronic environment around the sp^3 carbon not bonded to oxygen in our isomer is significantly different than in the other cyclobutanes and reflects a correspondingly different chemical shift tensor.

The observed (isotropic) chemical shift δ_{iso} is the average of the three principal values of the chemical shift tensor, which lie along three mutually perpendicular directions. Thus, if one or more of the principal values are unusually deshielded, this will be reflected in the observed chemical shift. The chemical shift tensor is well-known to be sensitive to local structure; modest changes in bond distances and bond angles can lead to variations in the calculated principal values of the chemical shift tensor and, therefore, in the isotropic chemical shift.[36] The relative similarity of the isotropic chemical shifts for the more downfield (and presumably oxygen-bound) sp^3 carbons in C_{2v} $C_{120}O_2$ (δ92.11) and our isomer (δ91.45) suggests that opposing changes in the principal values of the chemical shift tensor are occurring that nearly offset each other.

The structures shown in Figure 4 are also consistent with known examples of dimerization reactions among analogous anti-Bredt compounds, those with highly reactive, torsionally strained double bonds. The classic example in this class is the dimerization reaction of adamantene.[37]

Quantum Chemical Findings. To obtain a more detailed structural interpretation of experimental NMR data, we have performed extensive quantum chemical computations on each of the isomers shown in Figure 4. Approximate equilibrium geometries were found using the PM3 semiempirical method. Those structures were then refined through ab initio calculations that used DFT-B3LYP gradient-based geometry optimizations with basis sets of increasing size. Computational expense was minimized by the appropriate use of symmetry. Because of the large size of these molecules, we performed a full vibrational analysis at the DFT level only for the reference TMS molecule.

The B3LYP/3-21G* equilibrium geometries were then used for computations of ^{13}C NMR chemical shifts with the GIAO (B3LYP/3-21G* or B3LYP/6-31G*) ab initio method in Gaussian 98W. A study on taxol reported that GIAO computations

(29) Millar, J. M.; Creegan, K. M.; Robbins, J. L.; Robbins, W. K.; Sherwood, R. D.; Tindall, P. J.; Cox, D. M. *Synth. Met.* **1993**, *59*, 317−331.
(30) Giesa, S.; Gross, J. H.; Hull, W. E.; Lebedkin, S.; Gromov, A.; Gleiter, R.; Krätschmer, W. *Chem. Commun.* **1999**, 465−466.
(31) Knol, J.; Hummelen, J. C. *J. Am. Chem. Soc.* **2000**, *122*, 3226−3227.
(32) Dragoe, N.; Shimotani, H.; Hayashi, M.; Saigo, K.; de Bettencourt-Dias, A.; Balch, A. L.; Miyake, Y.; Achiba, Y.; Kitazawa, K. *J. Org. Chem.* **2000**, *65*, 3269−3273.
(33) Fujiwara, K.; Komatsu, K. *Chem. Commun.* **2001**, 1986−1987.
(34) Murata, Y.; Kato, N.; Komatsu, K. *J. Org. Chem.* **2001**, *66*, 7235−7239.
(35) Fujiwara, K.; Komatsu, K.; Wang, G.-W.; Tanaka, T.; Hirata, K.; Yamamoto, K.; Saunders: M. *J. Am. Chem. Soc.* **2001**, *123*, 10715−10720.
(36) Grant, D. M. *Encyclopedia of Nuclear Magnetic Resonance*; Wiley: London, 1996; Vol. 2, pp 1298−1321.
(37) Grant, D.; McKervey, M. A.; Rooney, J. J.; Samman, N. G.; Step, G. *Chem. Commun.* **1972**, 1186−1187.

Table 1. Comparison of Calculated and Experimental ^{13}C Chemical Shifts of sp^3 Atoms in Previously Studied Fullerene Compounds

compound	calculated chemical shifts (ppm) B3LYP/3-21G*	calculated chemical shifts (ppm) B3LYP/6-31G* (3-21G* geom)	measured chemical shifts (ppm)
$C_{60}O$ epoxide[10,29]	90.5	96.3	90.18[a]
C_{120}[2]	76.2	80.2	76.22[b]
$C_{120}O$[11]	78.7	82.4	78.9[b]
	97.9	102.7	99.0
$C_{120}O_2$ (C_{2v})[14]	73.2	76.2	72.19[c]
	91.4	96.1	92.11

[a] Measured in benzene-d_6 solution. [b] Measured in ODCB-d_4 solution. [c] Measured in 98:2 $CS_2/CDCl_3$ solution.

Table 2. Pairs of ^{13}C sp^3 Chemical Shift Values (in ppm) Computed for Five Possible $C_{120}O_2$ Isomers at Two Levels of Theory and the Values Measured Experimentally

$C_{120}O_2$ isomer	B3LYP/3-21G* (3-21G* geom)		B3LYP/6-31G* (3-21G* geom)	
C_2 (a)	81.2	88.2	85.8	93.0
C_2 (b)	83.2	92.9	86.9	98.5
C_i	86.3	96.1	90.0	101.9
C_s	81.8	100.1	86.3	105.2
C_i (+1)	72.2	74.1		
observed values	82.25	91.45	82.25	91.45

can predict ^{13}C chemical shifts within an accuracy of several ppm even with HF/6-31G* wave functions, and DFT-B3LYP wave functions can provide still better results.[38] Several investigators have also reported successful computations of ^{13}C NMR chemical shifts for some fullerene derivatives.[39,40] We ran calibration calculations on previously characterized fullerene oxides and dimeric fullerenes to assess the method's reliability for such compounds. We paid special attention to sp^3 chemical shift values, with the goal of using the two widely spaced experimental signals in this region to distinguish among the possible $C_{120}O_2$ isomeric structures. As shown in Table 1, we found that the chemical shifts of sp^3 carbons in these model fullerene compounds were predicted quite accurately using the smaller basis set. We note that the experimental dependence of chemical shifts on solvent is weak enough (only 0.3 ppm difference between $C_{120}O$ in ODCB-d_4 and $CS_2-CD_3COCD_3$[11,12]) to neglect when comparing experimental and calculated values.

Table 2 compares the measured sp^3 chemical shifts of our new $C_{120}O_2$ isomer with values computed for various possible structures. The results point to the class of structures shown in Figure 4 because the computed chemical shifts for these structures differ from experiment by less than 10 ppm. By contrast, the sp^3 chemical shifts computed for the "C_i (+1)" isomer (representing the class of structures with oxygen atoms one bond further from the bridging site) differ substantially from the measured values. Such large discrepancies let us exclude that class of structures and indicate that the new $C_{120}O_2$ isomer has one of the structures shown in Figure 4. Moreover, the most likely candidates are the ones labeled C_2 (a) and C_2 (b) because their predicted chemical shifts lie closest to the measured values.

Another guide to the identity of the observed isomer comes from computed energies of formation. The results of our computations using several methods are listed in Table 3. The most stable isomer is predicted to be C_2 (a), with an energy lower than that of two monomers by 126 kJ mol^{-1} (from B3LYP/3-21G*). We find that the energies of C_i and C_s isomers are considerably higher than those of the two C_2 symmetry structures. This result plus the NMR chemical shift predictions of Table 2 let us rule out the C_s and C_i isomers, leaving the C_2 (a) and C_2 (b) structures as the remaining candidates, with C_2 (a) very slightly preferred on energetic grounds.

Table 3. Relative Energies (in kJ mol^{-1}) of $C_{120}O_2$ Isomers as Computed by Various Methods

isomer	AM1	PM3	B3LYP/3-21G*	B3LYP/6-31G* (3-21G* geom)
C_2 (a)	0	0	0	0
C_2 (b)	+37	−2	+12	+2
C_i	+109	+67	+72	+75
C_s	+102	+50	+108	+99

Table 4. Computed Dipole Moments and Experimental HPLC Retention Times (Measured under Controlled Conditions) for Several Dimeric Fullerenes and Fullerene Oxides

compound	computed dipole moment, B3LYP/3-21G* (Debye)	retention time on Buckyprep column (min)	retention time on PBB column (min)
C_{120}	0	7.3	17.4
$C_{120}O$	0.65	7.7	17.0
$C_{120}O_2$ (C_{2v})	1.02	8.3	15.1
$C_{120}O_2$ observed		8.1	19.0
$C_{120}O_2$ (C_2 (a))	0.01		
$C_{120}O_2$ (C_2 (b))	0.80		

Experimental observations of HPLC retention times provide further structural information about our $C_{120}O_2$ isomer. We used previously reported methods to synthesize small amounts of several dimeric fullerenes and fullerene oxides (C_{120}, $C_{120}O$, and $C_{120}O_2$ (C_{2v})).[3,12,14] Examination of the retention times of these species on Cosmosil 5PBB and Buckyprep columns reveals certain elution patterns. We find that compounds in this group elute in order of increasing molecular mass on the Buckyprep column. However, on the 5PBB column, their retention times (for similar mass) depend mainly on molecular dipole moment, with higher dipole moments giving shorter retention times. Table 4 shows the increasing order of retention times for C_{120}, $C_{120}O$, and $C_{120}O_2$ (C_{2v}) on the Buckyprep column and the reversed order on the PBB column. The lower rows of this table show retention times measured under the same conditions for our new $C_{120}O_2$ isomer, along with the dipole moment values computed for the C_2 (a) and C_2 (b) candidate structures. Although the dipole moment of the C_2 (a) isomer does not vanish by symmetry, our computations predict it to be very small. The long PBB retention time of the new isomer strongly suggests that it is essentially nonpolar, thereby favoring assignment to the C_2 (a) structure shown in Figure 4. Note that we have also observed HPLC and UV−vis evidence for the presence of a second isomer of the dimer with a shorter PBB retention time and a yield near 7% of the main one. This minor isomer may be the C_2 (b) species.

Basic Photoproperties. The top frame of Figure 5 shows ground-state absorption spectra of $C_{120}O_2$ and [5,6]-$C_{60}O$, its monomeric precursor, in room-temperature toluene solutions prepared with equal mass concentrations. The near-UV peak

(38) Cheeseman, J. R.; Trucks, G. W.; Keith, T. A.; Frisch, M. J. *J. Chem. Phys.* **1996**, *104*, 5497−5509.
(39) Shimotani, H.; Dragoe, N.; Kitazawa, K. *J. Phys. Chem. A* **2001**, *105*, 4980−4987.
(40) Meier, M. S.; Spielmann, H. P.; Bergosh, R. G.; Haddon, R. C. *J. Am. Chem. Soc.* **2002**, *124*, 8090−8094.

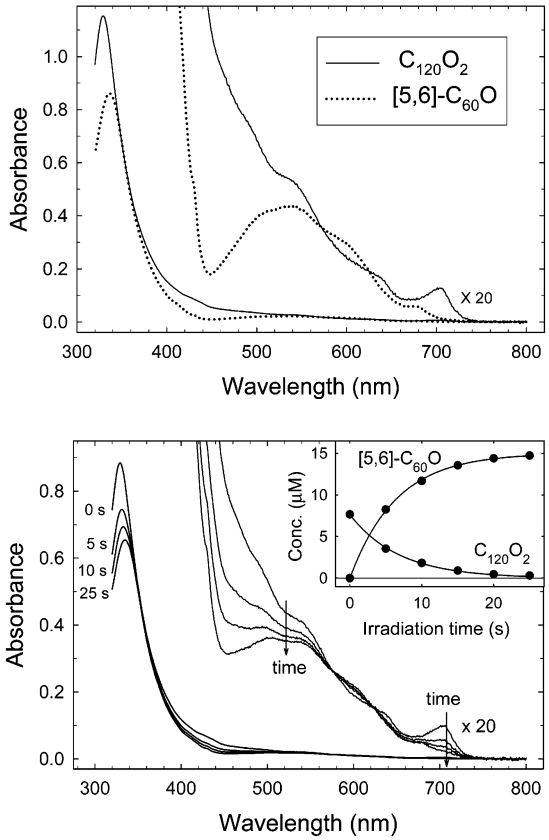

Figure 5. (Top frame) Absorption spectra of $C_{120}O_2$ (1×10^{-5} M) and [5,6]-$C_{60}O$ (2×10^{-5} M) in toluene. (Bottom frame) Spectral changes during photolysis of $C_{120}O_2$. The inset shows spectrophotometrically deduced concentrations of monomer and dimer species as a function of irradiation time.

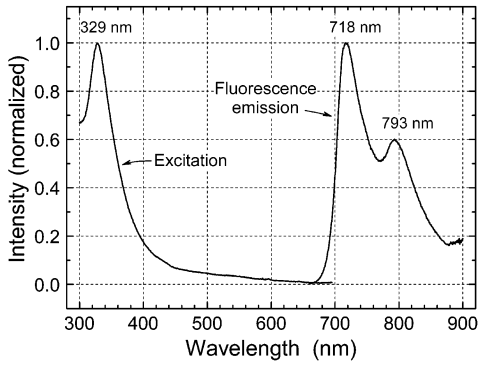

Figure 6. Fluorescence excitation and emission spectra of $C_{120}O_2$ in toluene.

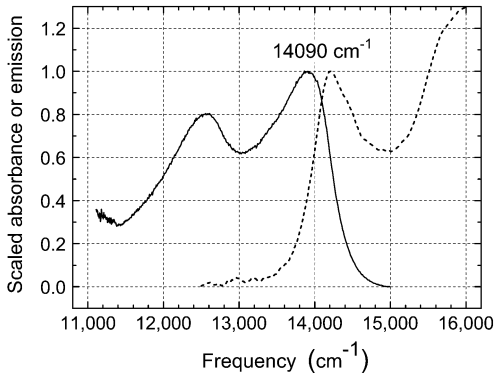

Figure 7. Absorption and fluorescence spectra of $C_{120}O_2$, transformed and overlaid to estimate the S_1 origin energy.

of the dimer lies at 329 nm, blue-shifted by approximately 6 nm relative to the monomer, and it lacks the monomer's absorbance minimum near 450 nm. Both of these differences reflect the presence of sp^3 derivatization sites only in the dimer. $C_{120}O_2$ also shows an $S_1 \leftarrow S_0$ absorption onset near 710 nm that is intensified and red-shifted by ca. 20 nm compared to the monomer.

Photophysical experiments on the new $C_{120}O_2$ isomer quickly revealed that the compound is chemically unstable when optically illuminated. In the lower frame of Figure 5, we show the changing absorption spectrum of a $C_{120}O_2$ sample during exposure to a photolyzing light source. The spectrum evolves into that of [5,6]-$C_{60}O$ during irradiation, and HPLC data confirm this photochemical conversion from dimer into monomers. The observed process resembles the photodissociation of C_{120} into C_{60} studied earlier in this laboratory.[9] We also found that the rate of $C_{120}O_2$ photodissociation is several orders of magnitude higher in degassed toluene solution than in aerated solution. This difference strongly suggests that dissociation occurs from the lowest triplet state, which is efficiently quenched by dissolved oxygen. The presence of isosbestic points near 572 and 624 nm indicates that the phototransformation of $C_{120}O_2$ involves no long-lived intermediate species. Because the absorbance change is also very minor near 360 nm, this spectral region can be considered nearly isosbestic. We therefore determined the molar absorptivity of the dimer using absorbance data at 360 nm and previous absorptivity results found for the monomer.[26] The molar absorptivity deduced for $C_{120}O_2$ is 115 000 ± 2000 M^{-1} cm^{-1} at the 329 nm peak.

To more accurately locate the S_1 origin energy of $C_{120}O_2$, we measured its fluorescence excitation and emission spectra. The measured excitation spectrum, shown in Figure 6, closely matches the compound's absorption spectrum, as expected. The emission spectrum has distinct maxima at 718 and 793 nm. In Figure 7, we show overlaid plots of $C_{120}O_2$ fluorescence and absorption spectra near 700 nm. To allow proper comparison, we have divided the absorbance values by frequency (ν), divided the emission intensities (in photons per second per unit frequency) by ν^3, and scaled the results to match amplitudes of the first peaks. The resulting very good mirror relation apparent in Figure 7 implies a value of 14 090 ± 70 cm^{-1} for the S_1-S_0 energy spacing of $C_{120}O_2$ in toluene.

Triplet State Photophysics. Studies of $C_{120}O_2$ triplet state properties were hampered by the tendency of samples to photochemically change composition during experimental runs. To suppress this problem, we measured triplet−triplet absorption kinetics using fewer than 10 low-power excitation pulses. Figure 8 shows such induced absorbance data acquired with a freshly prepared ~2.5×10^{-6} M sample, a probe wavelength of 715 nm, and averaging over only five excitation pulses. Kinetic analysis of this trace as a mixture of concurrent first- and second-order decays gave a first-order triplet state lifetime of 34 ± 2 μs for $C_{120}O_2$ in toluene at 298 K. As expected, second-order decay was found to be negligible. The 34 μs intrinsic triplet state lifetime is somewhat shorter than the value of 44 μs found earlier for C_{120} under comparable conditions,[9] but it is quite similar to the 31 μs triplet lifetime of [5,6]-$C_{60}O$.[26]

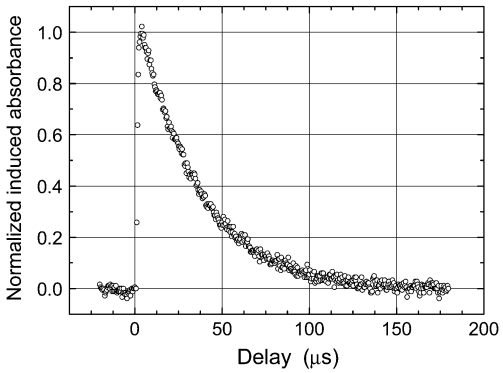

Figure 8. Triplet−triplet absorption kinetics of $C_{120}O_2$ in toluene at 297 K, measured at 715 nm following 532 nm pulsed excitation.

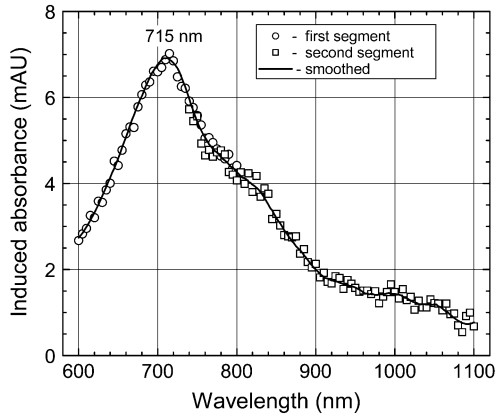

Figure 9. Induced (triplet−triplet) absorption spectrum of $C_{120}O_2$ in toluene following 532 nm excitation.

Because our measurements of transient absorption spectra are made by combining separate kinetic scans at many probe wavelengths, additional precautions were needed to ensure sample stability during such data acquisition. We used a stirred sample cell of relatively large volume (8 mL), reduced the excitation energy to ca. 0.04 mJ per pulse, and added enough oxygen to the sample to reduce the triplet state lifetime to approximately 6 μs, thereby lowering the photodissociative quantum yield. To scan the entire spectrum, we prepared two identical sample portions having concentrations near 4×10^{-6} M. The first portion was used for a scan from 600 to 800 nm in 5 nm steps, with a filter shielding the sample from shorter probe wavelengths. Then the second, fresh sample was scanned from 740 to 1100 nm with a different shielding filter. Only five excitation pulses were used at each probe wavelength, and HPLC sample analysis following the measurements confirmed that less than 10% of the dimer had been photolyzed. Figure 9 shows the resulting composite transient spectrum, in which the second data segment has been scaled by a factor of 0.98 to provide amplitude matching with the first. The spectrum shows a strong $T_n \leftarrow T_1$ maximum at 715 nm and a shoulder near 830 nm. Both of these features are typical of C_{60} adducts containing two adjacent sp^3 sites.[41]

We measured the quantum yield of triplet state formation by comparing the intensities of $^1O_2$ luminescence from absorbance-matched samples of $C_{120}O_2$ and C_{70} that were photoexcited in the presence of dissolved oxygen. The samples were saturated with O_2 at 1 atm in order to minimize photodissociation of $C_{120}O_2$ and to maximize the oxygen luminescence signals, which arose from energy transfer to oxygen during fullerene triplet quenching. HPLC analysis of the $C_{120}O_2$ samples after measurement showed less than 1% photodissociation. It was necessary to correct the observed oxygen luminescence signals for differences in $^1O_2$ lifetimes between the sample solutions (25 and 29 μs for the $C_{120}O_2$ and C_{70} samples, respectively). Taking the triplet quantum yield, Φ_T, of the C_{70} reference to be 1.0,[42] we then found that Φ_T of $C_{120}O_2$ equals 1.0 ± 0.1.

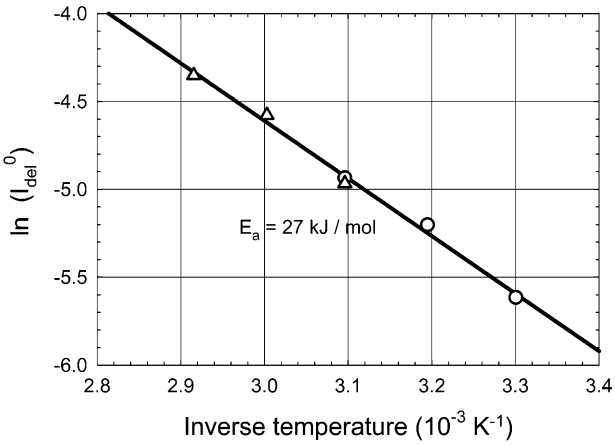

Figure 10. Arrhenius-type plot showing the temperature dependence of the intensity of initial delayed fluorescence. Symbols mark experimental data, and the solid line is a linear best fit.

Our attempts to directly determine the energy of the $C_{120}O_2$ T_1 state by phosphorescence spectroscopy were unsuccessful, so we instead used the indirect method of finding the S_1-T_1 energy gap through thermally activated delayed fluorescence (TADF) measurements and then combining this gap value with the spectroscopically determined S_1 energy to obtain the T_1 energy. The TADF measurements on $C_{120}O_2$ were unusually challenging because this compound seems to be photochemically unstable in polymer films, the preferred medium for such experiments. We prepared samples in fluid solution but had to suppress complications from triplet−triplet annihilation by using low concentrations, reduced excitation energies, and a paraffin/toluene solvent mixture with higher viscosity. To limit sample photolysis, we also restricted the number of excitation pulses and used a large volume cuvette with magnetic stirring. Measured intensities of delayed fluorescence were scaled to the prompt fluorescence amplitudes in order to compensate for any changes in sample concentration or temperature dependence in the fluorescence quantum yield. Figure 10 shows an Arrhenius-type plot of the measured delayed fluorescence intensity. From the linear least-squares fit, we find an activation energy of 27 kJ/mol ($\sim$2300 $\pm$ 200 cm^{-1}), which represents the S_1-T_1 energy gap. This value is consistent with an independent determination based on the ratio of delayed and prompt fluorescence intensities in our sample.[43] We therefore deduce that the T_1 origin lies 11 800 $\pm$ 200 cm^{-1} above the ground state.

(41) Weisman, R. B. Optical Studies of Fullerene Triplet States. In *Optical and Electronic Properties of Fullerenes and Fullerene-Based Materials*; Shinar, J., Vardeny, Z. V., Kafafi, Z. H., Eds.; Marcel-Dekker: New York, 2000; pp 83−117.

(42) Berberan-Santos, M. N.; Garcia, J. M. M. *J. Am. Chem. Soc.* **1996**, *118*, 9391−9394.

(43) Bachilo, S. M.; Benedetto, A. F.; Weisman, R. B.; Nossal, J. R.; Billups, W. E. *J. Phys. Chem. A* **2000**, *104*, 11265−11269.

Dissociative Photochemistry. Initial data on photodissociation kinetics were obtained from HPLC analyses of irradiated $C_{120}O_2$ solutions. A set of replicate samples was prepared, carefully degassed, and then photolyzed for various times with 532 nm pulses from a Nd:YAG laser. To ensure homogeneous irradiation, we used a defocused laser beam, a low pulse repetition rate (~1 Hz), and magnetic sample stirring. HPLC analysis then provided reactant and product concentrations as a function of irradiation time. The resulting $C_{120}O_2$ concentrations showed first-order decay with a constant, $k_{transform}$, of 0.001 67 s^{-1}. To convert this value into a photochemical quantum yield, we applied the following relation (valid for optically thin samples):

$$\Phi_{diss} = \frac{k_{transform} N}{2.303 A P_0} \quad (1)$$

where N is the total number of sample molecules in the cell, A is the initial absorbance at the photolysis wavelength, and P_0 is the incident laser power in photons per second. Evaluating eq 1 with our experimental parameters, we found that $C_{120}O_2$ in degassed toluene at 297 K has a quantum yield for photodissociation of 0.025.

Although quite accurate, this method for measuring the photochemical quantum yield is tedious. For further measurements we applied a simpler method based on the difference in molar absorptivities between the monomer and dimer. At 329 nm, the absorbance of a $C_{120}O_2$ solution decreases by approximately 30% when it dissociates into two monomers. The concentration change of the dimer can therefore be found from ΔA, the absorbance change, using the following expression:

$$\Delta[C_{120}O_2] = \frac{\Delta A^{329}}{(\epsilon^{329}_{C_{120}O_2} - 2\epsilon^{329}_{C_{60}O}) l} \quad (2)$$

We measured 329 nm absorbance changes as a function of irradiation time to find $k_{transform}$ at various sample temperatures. Analysis using eq 1 then confirmed the quantum yield value deduced from HPLC data and also showed that Φ_{diss} increases sharply, from 0.025 to 0.425, between 297 and 343 K.

To investigate this variation in photodissociative quantum yield, we made temperature-dependent measurements of induced absorption kinetics over the same range, using the procedure described earlier. These results showed that the triplet state decay constant, k_T, also varies strongly with temperature. Measured k_T values are plotted in the top frame of Figure 11. Also plotted in this figure are the rate constants for dissociation of triplet state $C_{120}O_2$, k_{diss}, which were obtained by dividing the temperature-dependent Φ_{diss} values by the corresponding triplet state lifetimes. Over the studied temperature range, this dissociation rate constant varies from 730 to 19 600 s^{-1}. The final trace in the top frame of Figure 11 shows the difference between k_T and k_{diss}, which we identify as k_{ISC}, the rate constant for $T_1 \rightarrow S_0$ radiationless decay. It can be seen that the photophysical relaxation represented by k_{ISC} has very little temperature dependence over the studied range.

In the lower frame of Figure 11, we show an Arrhenius plot of the deduced dissociation rate constants along with a linear best fit. The slope implies an activation energy for triplet state dissociation of 60 kJ mol^{-1} (5000 cm^{-1}). The Arrhenius prefactor is approximately 2.3×10^{13} s^{-1}, corresponding to an attempt frequency near 800 cm^{-1}. These values indicate that once $C_{120}O_2$ reaches the T_1 state, it can undergo vibrationally activated dissociation over a modest potential barrier to regenerate [5,6]-$C_{60}O$.

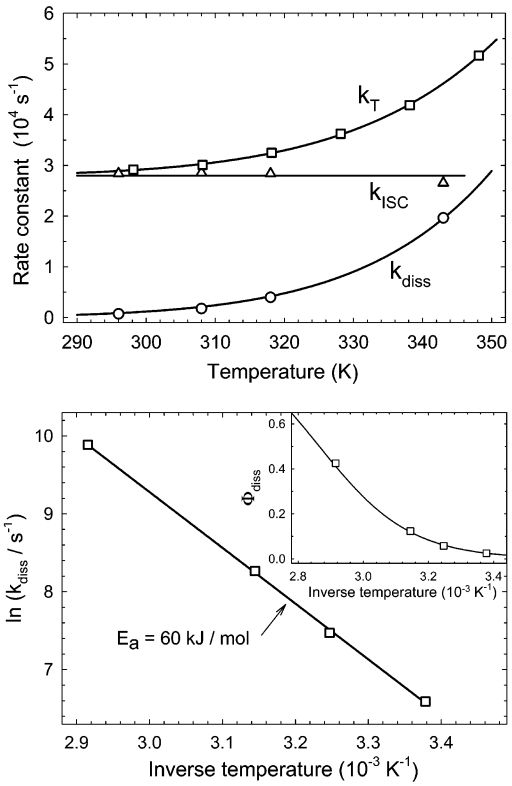

Figure 11. (Top frame) $C_{120}O_2$ temperature-dependent rate constants for overall triplet state decay (k_T), $T_1 \rightarrow S_0$ intersystem crossing (k_{ISC}), and triplet state dissociation (k_{diss}). (Bottom frame) Arrhenius plot of k_{diss}. (Inset) Temperature variation of Φ_{diss}, the photodissociation quantum yield.

Conclusions

We have found that the recently discovered oxidoannulene isomer of $C_{60}O$ readily dimerizes in room-temperature solution to form a new isomer of $C_{120}O_2$. The $C_{120}O_2$ product contains a four-membered bridging ring, as in C_{120}, and has C_2 symmetry. When optically excited, this dimer undergoes intersystem crossing to populate its triplet state with near-unit efficiency. The $C_{120}O_2$ triplet state lies 11 800 cm^{-1} above its ground state, shows an intrinsic lifetime of 34 μs (at 24 °C), and has an absorption peak at 715 nm. All of these values are typical for C_{60} monoadducts. However, the triplet state also undergoes unusual thermally activated dissociation to regenerate the [5,6]-$C_{60}O$ precursor with quantum yields that reach 43% at 70 °C. These compounds therefore form the first fullerene system containing monomers and dimers in a dynamic balance that can be easily controlled through adjustment of concentration, temperature, and light exposure.

This new isomer of $C_{120}O_2$ should prove useful as a stable reactant for the convenient photolytic generation of [5,6]-$C_{60}O$. The high reactivity found for [5,6]-$C_{60}O$ in this initial study of its chemical behavior apparently arises from the strained sp^2

bonds adjacent to the oxygen atom. The ability of [5,6]-$C_{60}O$ to undergo chemical reactions under mild conditions may make it an attractive reactant for the synthesis of novel nano-bio conjugates.

Acknowledgment. We are grateful to Dr. T. Marriott for expert mass spectrometry assistance. This research has been supported by the National Science Foundation (Grants CHE-0314270 and CHE-9708978) and the Robert A. Welch Foundation (Grant C-0807).

Supporting Information Available: Table of ^{13}C NMR shifts (in ppm) observed for $C_{120}O_2$ in *o*-dichlorobenzene-d_4. This material is available free of charge via the Internet at http://pubs.acs.org.

JA048937D